INTERFACE SCIENCE 1, 49–60 (1993).

Theoretical Aspects of Solute Segregation to High-Angle Grain Boundaries

J.O. VASSEUR, P.A. DEYMIER*, B. DJAFARI-ROUHANI, AND L. DOBRZYNSKI
Equipe de Dynamique des Interfaces, Laboratoire de Dynamique et Structure des Matériaux Moléculaires, U.R.A. C.N.R.S. n°801-U.F.R. de Physique, Université dé LILLE I, 59655 VILLENEUVE d'ASCQ, Cédex-FRANCE

Received October 21, 1992; Revised February 1, 1993.

Keywords: Segregation, grain boundaries, enrichment factor.

Abstract. A high-angle grain boundary is modeled as a planar defect characterized by its thickness and atomic density. We successively examine the elastic and electronic contributions to the solute/grain boundary binding energy. We deduce the effect of the grain boundary physical parameters on its propensity for segregation. The thickness of high-angle grain boundaries is not a fundamental parameter for segregation. The atomic density in the grain boundary controls the electronic binding energy. The rate of change of elastic constants with the density is the important factor in the elastic contribution to segregation. We conclude that segregation to boundaries with small excess volumes is not precluded.

1. Introduction

Equilibrium segregation at grain boundaries is an important phenomenon in view of the many drastic and sometime detrimental effects it may induce on the physical properties of polycrystalline materials. Segregation in alloys occurs by concentration or depletion of the solute in the vicinity of grain boundaries. The extent of segregation has been observed by modern analytical technics such as Auger microprobe [1] or field ion microscopy [2] to be limited to only a few atomic layers adjacent to the boundary or even a monolayer. It is also recognized that the extent of solute segregation is affected by the physical characteristics of the grain boundaries. For instance, in Fe-S alloys it was revealed that the amount of sulfur segregation increases with the misorientation angle from small values to the high-angle regime [3]. Low-angle grain boundary can be represented by arrays of dislocations. Segregation at these boundaries arises from the interactions between the solute atoms and the elastic strain field of the dislocations [4]. Less is known about the relation between structure and propensity for segregation in the case of high-angle grain boundaries. A dependency of segregation on the crystallographic orientation of the boundary has been observed in Fe-P alloys [5]. Large amounts of phosphorus segregate to grain boundaries with high crystallographic indices, while the extent of segregation is smaller to low-indices planes. There appears to exist a relation between segregation propensity and the character of high-angle grain boundaries. One classifies boundaries into "special" boundaries and "general" boundaries on the basis of the degree of matching between the adjoining lattices. The special grain boundaries with higher degree

*Permanent Address: Department of Materials Science and Eng., University of Arizona, Tucson, AZ 85721, USA.

of order are often referred to as low energies. Special boundaries in Ni, as measured by the density of coincident sites Σ, have shown weak tendency for sulphur segregation [6]. Furthermore, in other experiments, a relation was found between segregation and grain boundary energy [7, 8] with least impurity content at low-energy boundaries. However, an evidence of segregation of Re in a low-energy grain boundary in W exists [2].

On the other hand, experimental measurements of segregation in several metals have demonstrated a correlation between the grain boundary enrichment and the solubility of the solute [9]. The enrichment factor defined as the ratio of the grain boundary solute content and the bulk content is inversely proportional to the solute solubility limit [10].

A variety of theoretical models for equilibrium segregation rely on a Gibbsian description of a bicrystal separated into grain boundary and bulk regions [11, 12]. These theories result in a segregation isotherm with limited predictive ability regarding the local chemical and structural states of the system. Thus they are unable to provide an equilibrium solute concentration as a function of distance from the grain boundary. A recent mean-field theory of segregation [13] proposed a finer division of the crystal for unidimensional chemical and structural predictions at the atomic scale.

The study of segregation in alloys at the microscopic scale has gained from realistic atomistic computer simulation techniques [14, 15]. The degree of realism of these calculations depends on the use of potentials to describe the interactions between atomic species. They also permit a clear description of the structural character of the grain boundaries studied, allowing the investigation of the relationship between the structure of the interface and segregation.

With finer models including the atomic structure of grain boundaries, one gains in realism but one may lose in practicality. Indeed, the difficulties of implementation of such models render their application to the study of the very large multiplicity of grain boundaries quite elusive. Wolf [16] has shown (based on a large number of computer simulations of grain boundaries in various metals) that a limited set of physical parameters, such as the interface excess volume, are related to the energy of high-angle grain boundaries. This result suggests that there may not be any need to know the structure of a grain boundary in detail, but that some more macroscopic variables may be used in place.

In the hope that a similar reasoning can be extended to the problem of grain boundary segregation, we propose in this paper to develop a practical approach to modeling the phenomenon of segregation to high-angle grain boundaries in simple metals. In this approach, the core of a high-angle grain boundary is essentially constituted of a stress-free thin slab of "bad" material sandwiched between two perfect crystals. The physical characteristics of the grain boundary are parametrized through a small number of variables associated with the core region. Thickness and excess volume are the two basic parameters in the model.

In simple metals, the driving forces for equilibrium segregation include the reduction of excess energy by accomodation of the excess mechanical strain or electronic mismatch from solutes that fit poorly in the host material [4]. We calculate the solute/boundary binding energy within the frame of linear elasticity. An extension of the method for the determination of solute/boundary excess elastic energy to the electronic contribution within a free electron model is straightforward for simple metals. The elastic contribution to the binding energy is thus incorporated into a local isotherm theory, which permits the derivation of segregant concentration profiles and grain boundary enrichment. Most significantly in this work is the possibility of relating chemical information to the high-angle grain boundary structural parameters.

In section 2, we derive the isotherm theory for the calculation of a theoretical solute concentration profile. Sections 3 and 4 contain the determination of the elastic and electronic contributions to the solute binding energy in relation to the grain boundary structural variables. The effect of these structural parameters on segregation are also reported. Finally, in section 5 some conclusions are drawn regarding the relationship between segregation propensity and the physical character of high-angle grain boundaries.

2. Local Isotherm Theory

We initially define the geometric model of a high-angle grain boundary. The thin slab of bad material can be considered like a planar defect B sandwiched between two semi-infinite media A. The slab is centered on $X_3 = 0$, where X_3 is a direction perpendicular to the interfaces; these ones localised on $X_3 = \pm a$.

To develop a local isotherm theory, we divide the semi-infinite medium A into thin planar regions parallel to the grain boundary. The location of each planar region is identified by the integer parameter l. Then, the energy of interaction of impurities with the grain boundary takes the form

$$E = N \sum_{l} \rho(l) E_l(l), \tag{1}$$

where $\rho(l)$ is the fraction of atomic sites in the slab l occupied by impurities; $E_l(l)$ is the position dependent binding energy of one impurity with the grain boundary; and N is the number of atomic sites in each plane parallel to the grain boundary.

On the other hand, there is a configurational entropy $s(l)$ in each plane l [$N\rho(l)$ sites are occupied among the N existing sites]

$$s(l) = k_B \mathrm{Ln} \frac{N!}{(N\rho)![N(1-\rho)]!}, \tag{2}$$

where k_B is the Boltzmann constant.

For large N, equation (2) leads to

$$S = \sum_{l} s(l)$$

$$= -k_B N \sum_{l} [\rho \mathrm{Ln}\rho + (1-\rho)\mathrm{Ln}(1-\rho)]. \tag{3}$$

We have to minimize the Helmotz free energy $F = E - TS$ with respect to the $[\rho(l)]$ under the condition

$$\sum_{l} \rho(l) = \text{constant}. \tag{4}$$

By introducing a Lagrange multiplier λ, we obtain

$$E_l(l) + k_B T \mathrm{Ln} \frac{\rho}{1-\rho} - \lambda = 0. \tag{5}$$

For large l, formula (5) gives for λ

$$\lambda = k_B T \mathrm{Ln} \frac{\rho_b}{1-\rho_b} \tag{6}$$

where ρ_b is the impurity concentration in the bulk; then equation (5) reduces to

$$E_l(l) + k_B T \mathrm{Ln} \frac{\rho}{\rho_b} \frac{1-\rho_b}{1-\rho} = 0 \tag{7}$$

or

$$\rho = \frac{\rho_b \exp(-E_l/k_B T)}{1 - \rho_b + \rho_b \exp(-E_l/k_B T)}. \tag{8}$$

This Langmuir adsorption type equation applied to the case of grain boundary segregation was originally derived by McLean [11] for a fixed value of binding energy independent of position. In the limit of low concentration ρ_b, and energy E_l not much greater than a few $k_B T$, the Langmuir-McLean equation (8) reduces to a locally varying isotherm

$$\rho \simeq \rho_b \exp(-E_l/k_B T). \tag{9}$$

Let us now calculate the elastic contribution to the binding energy E_l.

3. Elastic Contribution to the Binding Energy

In the case of solutions of isovalent metals, size effects, and therefore elastic strain, may provide the essential part of the driving force for segregation [17]. Assuming full relaxation of strain energy at the interface, McLean [11] has used an expression for the elastic energy of a sphere inserted in a cavity of smaller radius derived by Pines [18] to estimate the segregation-binding energy.

Here, an impurity atom is described within the Leibfried's model [19] in which a spherically symmetric point defect is represented by a superposition of three perpendicular double forces without moment centered at a point X_0. This distribution of forces is written as

$$F_\alpha(\mathbf{X}) = -A_0 \frac{\partial}{\partial X_\alpha} \delta(\mathbf{X} - X_0), \quad \alpha = 1, 2, 3 \tag{10}$$

where A_0 is a constant with the dimension of a force times length.

The strain energy associated with the intro-

duction of this body force is given by [20]

$$U_s = \frac{1}{2}\sum_{\alpha,\beta}\int d^3X \int d^3X' F_\alpha(\mathbf{X}) \; g^0_{\alpha\beta}(\mathbf{X}, \mathbf{X}')F_\beta(\mathbf{X}'), \tag{11}$$

where $g^0_{\alpha\beta}(\mathbf{X}, \mathbf{X}')$ is the Green function of the medium. In the case of a point defect inserted into an *A-B-A* sandwich model of a bicrystal, the translational symmetry parallel to the planar defect permits a Fourier analysis of the Green function in the form

$$g^0_{\alpha\beta}(\mathbf{X}, \mathbf{X}') = \int \frac{d^2k_{//}}{(2\pi)^2} g^0_{\alpha\beta}(k_{//}|X_3, X_3') \times \exp[i\mathbf{k}_{//}.(\mathbf{X}_{//} - \mathbf{X}'_{//})], \tag{12}$$

where $\mathbf{k}_{//}$ and $\mathbf{X}_{//}$ are both two-dimensional vectors with components $(k_1, k_2, 0)$ and $(X_1, X_2, 0)$.

For a medium isotropic in planes perpendicular to X_3, the Green function can be further expressed in terms of simpler coefficients by rotating the vector $\mathbf{k}_{//}$ into a vector $(k_{//}, 0, 0)$ with the transformation

$$S(k_{//}) = \begin{pmatrix} \frac{k_1}{k_{//}} & \frac{k_2}{k_{//}} & 0 \\ -\frac{k_2}{k_{//}} & \frac{k_1}{k_{//}} & 0 \\ 0 & 0 & 1 \end{pmatrix}. \tag{13}$$

The Green function is written in the form

$$g^0_{\alpha\beta}(\mathbf{k}_{//}|X_3, X_3') = \sum_{\mu,\nu} S^{-1}_{\alpha\mu}(k_{//}) \; g_{\alpha\beta}(\mathbf{k}_{//}|X_3, X_3')S_{\nu\beta}(k_{//}), \tag{14}$$

and the strain energy becomes

$$U_s = \frac{1}{2}\sum_{\mu,\nu}\int \frac{d^2k_{//}}{(2\pi)^2}\int dX_3 \int dX_3' f_\mu(\mathbf{k}_{//}|X_3) \times g_{\mu\nu}(k_{//}|X_3, X_3')f^*_\nu(\mathbf{k}_{//}|X_3'), \tag{15}$$

where

$$f_\mu(\mathbf{k}_{//}|X_3) = \sum_\alpha S_{\mu\alpha}(k_{//}) \int d^2\mathbf{X}_{//} F_\alpha(\mathbf{X}) \times \exp(i\mathbf{k}_{//}.\mathbf{X}_{//}). \tag{16}$$

The * in equation (15) denotes the complex conjugate.

The $f_\mu(\mathbf{k}_{//}|X_3)$'s of the symmetrical point defect defined in equation (16) are

$$f_1(\mathbf{k}_{//}|X_3) = iA_0k_{//}\delta(X_3 - X_{03})\exp(i\mathbf{k}_{//}.\mathbf{X}^{(0)}_{//}) \tag{17}$$

$$f_2(\mathbf{k}_{//}|X_3) = 0 \tag{18}$$

$$f_3(\mathbf{k}_{//}|X_3) = -A_0\frac{d}{dX_3}\delta(X_3 - X_{03}) \times \exp(i\mathbf{k}_{//}.\mathbf{X}^{(0)}_{//}), \tag{19}$$

where $\mathbf{X}^{(0)}_{//}$ is the position of the point defect in a plane perpendicular to X_3.

Let us denote by C_{11}, C_{44} and C'_{11}, C'_{44} the elastic constants of the isotropic media *A* and *B*. The point defect is located in the left semi-infinite medium at a distance X_{03} from the center of the slab.

The Green function, *g*, of the *A-B-A* sandwich is the sum of the Green function of an infinite medium, G_∞, and of the contribution of the interfaces between media *A* and *B*, $G = g - G_\infty$. The two dimensional Fourier transform of the Green function, $G(k_{//}|X_3, X_3')$, in the region $X_3 \leq -a$ and $X_3' \leq -a$ was reported in a previous publication [21].

The energy of interaction, U_s, between the impurity and the planar defect is determined by inserting *G* into equation (15). This energy is obtained in the form

$$U_s = \frac{A_0^2}{8\pi C_{11}^2}\int_0^{k_D} dk_{//}k_{//}\exp(-2k_{//}|X_{03}|)\phi(k_{//}). \tag{20}$$

The upper limit, k_D [22], for the integration over $k_{//}$ arises from the inability of continuous elasticity to represent the discrete nature of crystal lattices [23]. The function $\Phi(k_{//})$ is given in an appendix.

The energy U_s was calculated analytically in the limit of a very thin slab [21]. It was given as

$$U_s = \frac{A_0^2}{16\pi C_{11}}\frac{\nu\nu'}{(1+\nu)}\frac{a}{|X_{03}|^4} \times \left[1 - \frac{h_{11}(1+\nu')}{h_{44}^2(1+\nu)}\right] I_3(\xi), \tag{21}$$

where we defined $\nu = C_{44}/C_{11}$; $\nu' = C'_{44}/C'_{11}$; $h_{11} = C'_{11}/C_{11}$; and $h_{44} = C'_{44}/C_{44}$. We also used the notation

$$I_3(\xi) = \int_0^\xi du\, u^3\exp(-u), \quad \xi = 2k_{//}|X_{03}|. \tag{22}$$

This energy varies as the inverse fourth power of the distance from the planar defect in agreement with earlier calculation based on a capillary method [24]. The energy of interaction is proportional to the thickness of the planar defect and may change sign depending upon the ratio of elastic constants in both media A and B.

Here, we integrate numerically equation (20) considering the constant A_0 as an unknown quantity, to investigate the full dependency of the interaction energy upon the thickness of the slab and the position of the point defect. Since the energy U_s is a quadratic function of the constant A_0, its sign depends only on the values of the elastic constants. Therefore, we place ourself in the case of a negative energy, that is, C'_{11} and C'_{44} less than C_{11} and C_{44}, respectively. These values are rationalized on the basis of lower atomic densities in the core of high-angle grain boundary [25]. We find that the energy of interaction is short range.

For the sake of quantitative comparison with available experimental information, we focus our attention on the calculation of the grain boundary enrichment factor. We take the value of the interaction energy at $X_{03} = -a$ as representative of the impurity/grain boundary binding energy. As remarked by Smith and Ferrante [26], the magnitude of the thickness of high-angle grain boundaries is on the order of 5 Å. Therefore, the elastic energy of the point defect within the slab cannot be taken as the binding energy in view of the limitation of continuous elasticity to calculating the phenomenon at an atomic scale [23].

Using equation (9), the grain boundary enrichment factor, β, is defined as

$$\beta = \frac{\rho(-a)}{\rho_b} = \exp\left[-\frac{U_s(-a)}{k_B T}\right]. \tag{23}$$

Hondros [9] obtained experimentally, for various metallic alloys, a linear relationship between $\mathrm{Ln}\beta$ and the logarithm of the solute solubility limit X_s. A slope of approximately -1 appears to correlate $\mathrm{Ln}\beta$ and $\mathrm{Ln}X_s$; this is for several solvents or crystalline form of the same solvent.

We estimate the elastic contribution to the limit of solubility for impurities of low solubility from the relation [10, 27]

Table 1. Input values for the calculation of the ratio R given in Fig. 2.

	$C_{11}(10^{11}\ \mathrm{N/m^2})$	$C_{44}(10^{11}\ \mathrm{N/m^2})$	$k_D(10^{10}\ \mathrm{m^{-1}})$
W	5.120	1.530	1.23
Al	1.113	0.261	0.96

$$X_s = \exp\left[-\frac{U_\infty}{k_B T}\right]. \tag{24}$$

In this equation, the energy U_∞ is the elastic energy of a spherical point defect embedded in an infinite isotropic medium of elastic constants C_{11} and C_{44}. This energy was calculated from the Green function of an infinite isotropic elastic medium [20] in the form [28]

$$U_\infty = \frac{A_0^2 k_D^3}{12\pi^2 C_{11}}. \tag{25}$$

As remarked by Friedel [17], in the case of solutions of isovalent metals, the elastic contribution, X_s, to the limit of solubility approaches the exact limit.

Finally, eliminating the strength of the impurity's distribution of forces A_0 between equations (23) and (24) yields the theoretical linear relation linking $\mathrm{Ln}\beta$ and $\mathrm{Ln}X_s$. Only grain boundary and bulk physical parameters enter this relationship.

In figure 1, we report the variation of the ratio $R = \mathrm{Ln}\beta/\mathrm{Ln}X_s$ with the half-thickness of the grain boundary for two types of metals, tungsten and aluminium. Tungsten is a transition metal for which the assumption of isotropicity is justified, while aluminium is a nonisotropic simple metal.

The grain boundary core density is approximately 0.9 times that of the bulk [26]. We calculate the elastic constants of the core as a function of density from relations between the elastic constants and density of the bulk with temperature [29]. The elastic constants are then given as linear functions of the atomic density. For this grain boundary core density, the elastic constants C'_{11} and C'_{44} are 0.4 times those of the bulk. All the physical constants used in this calculation are listed in table 1.

These estimates are only approximate in the sense that the elastic constants only depend on density. It is clear, however, that crystallographic arguments should also control the values of the

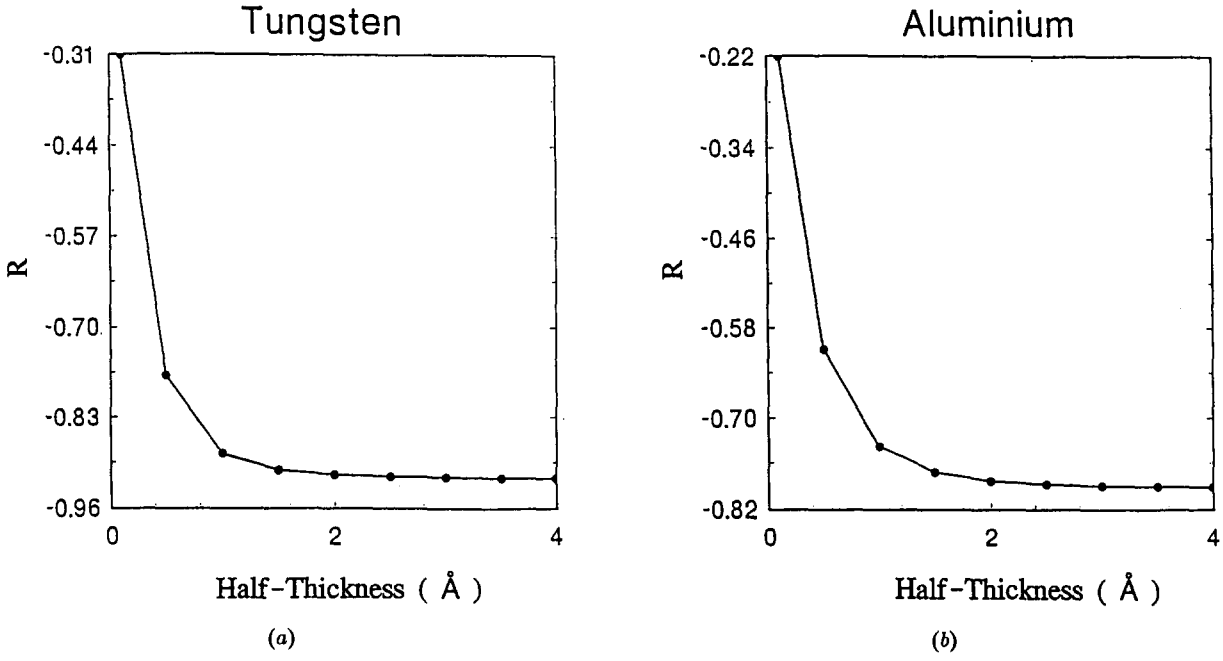

Fig. 1. Variation of the ratio R with the half-thickness of the grain boundary for two types of metals. (*a*) In the case of tungsten; (*b*) In the case of aluminium.

grain boundaries elastic constants. It would be, therefore, necessary to perform precise calculations of grain boundaries elastic constants as done by Wolf and Lutsko [30] with computational methods. In their atomistic simulation of high-angle grain boundary in gold with 4% excess volume, Wolf and Lutsko calculated a reduction of 17% and 97% in the grain boundary elastic constants C'_{11} and C'_{44}. These numbers show that our estimation of the elastic constants for a grain boundary with 10% excess volume is reasonable.

In figure 1, we observe that, in both cases, the ratio R shows drastic changes with the thickness in the range 0–3 Å.

It remains nearly constant for thicknesses greater than 4 Å. In this latter regime, which corresponds to typical high-angle grain boundaries, this ratio takes a value approaching the experimental slope of -1. This result is also in accord with a solid-solid interface analogue [27] of a theory of adsorption [31].

The weak dependency of R on the thickness above 3 Å is understandable on the basis of a smaller contribution to the binding energy of one of the interfaces between the slab and a semi-infinite medium. In the limit of unphysically large thicknesses, the problem reduces to the interaction of a point defect with an interface between two isotropic elastic media [32].

An alternative model of a high-angle grain boundary is an interface between two semi-infinite media. In an anisotropic crystal, the solute atom sees the misoriented half-crystal in which it does not reside with average elastic constants different from those of the host half-crystal [33]. In this case, the energy of interaction varies as the inverse of the cube of the distance. The major drawback of the model of a single interface between two semi-infinite media is that it does not allow the characterization of a grain boundary as a separate entity with its own physical characteristics.

The grain boundary density affects the ratio, R, through variations in C'_{11} and C'_{44}. We plot in figure 2, R versus $h_{11} = C'_{11}/C_{11}$ (assuming a similar variation for C'_{44}/C_{44} [29]). We choose a constant value of 5 Å for the thickness of the planar defect. All other physical constants are those of aluminium (See table 1).

Two trivial cases are obtained for $h_{11} = 1$ and 0. The former corresponds to a perfect

crystal without sites for segregation. The latter gives the free surface. A value for the ratio R on the order of -2.25 indicates a strong propensity for surface segregation of low solubility solute. For typical values of atomic densities in high-angle grain boundaries (15–5% lower than the bulk), h_{11} takes values between 0.4 and 0.3. This corresponds to ratios R varying in the range -0.8 to -1.1.

It is worthy noting the insensitivity of the ratio R on the physical parameters of typical high-angle grain boundaries such as thickness. Furthermore, this ratio is independent of the solute character, as represented by the constant A_0. This may explain the remarkable empirical correlation between grain boundary enrichment factor and solubility derived by Hondros [9] for a very wide range of systems.

We observe also that the elastic binding energy is indirectly linked to the grain boundary atomic density through the elastic constants. The important quantity here is h_{11}. Assuming a linear variation between elastic constants and density, we write :

$$h_{11} = S(d_B - d_A)/C_{11} + 1 \tag{26}$$

where d_B and d_A are grain boundary and bulk atomic densities. S represents the variation of the elastic constants with density. It is a material property that determines the elastic contribution to segregation.

This suggests a possibility of strong segregation to grain boundaries with atomic densities approaching the bulk value. Consider the same boundary (as described by the grain misorientation and the crystallographic indices of the boundary plane) in two simple metals M_1 and M_2. Let S_1 and S_2 be the elastic constants variations with density of the two metals, respectively. We assume that S_1 is much larger than S_2 and that the grain boundary density differs only slightly from the bulk value. The elastic contribution to segregation will be much greater for the metal M_1 than for the metal M_2. Indeed, the small density variation in the boundary gives rise to a significantly lower value for h_{11} in the case of metal M_1 than in the case of metal M_2. A small value of h_{11} results in a strong grain boundary enrichment factor. This explains why a grain boundary with little excess volume may exhibit a high adsorptive capacity for solutes.

4. Electronic Contribution to the Binding Energy

In metallic alloys of heterovalent elements [17], segregation is driven not only by the elastic misfit but also by valence effects. The purpose of this section is to obtain within a simple model the excess electronic energy of a point defect near a planar defect modeled again as a thin slab of metal B sandwiched between two semi-infinite perfect crystals of metal A. The calculations are conducted in the nearly free electron model, with step barriers at the interfaces, and are based on the Green function method [34]. The nearly free electron approximation limits the applicability of the model to simple metals.

We model a solute atom located at $\mathbf{r}_0$ as a perturbing potential of the form [35]

$$V(\mathbf{r}) = A\delta(\mathbf{r} - \mathbf{r}_0), \tag{27}$$

where $\delta(\mathbf{r})$ is the usual delta function, and A defines the strength of the perturbation. We consider the case of a small perturbation.

Therefore, the correction to a non-degenerated electronic energy level of the system due to this potential is written, to first order in the perturbation $V(\mathbf{r})$, in the form

$$\epsilon(\mathbf{r}_0, E) = < \Psi | V | \Psi >, \tag{28}$$

where $| \Psi >$ is an eigen vector of the unperturbed system associated with the energy E. Introducing equation (27) in equation (28) gives

$$\epsilon(\mathbf{r}_0, E) = An_0(\mathbf{r}_0, E). \tag{29}$$

The expression $n_0(\mathbf{r}_0, E)$ is the contribution of the electrons with energy E to the electronic density at location $\mathbf{r}_0$ in the unperturbed sandwich system.

Furthermore, the electronic density $n_0(\mathbf{r}_0, E)$ can be advantageously determined from the imaginary part of the Green function, $g(\mathbf{r}_0, \mathbf{r}_0, E)$ of the unperturbed system by the relation

$$n(\mathbf{r}_0, E) = -\frac{1}{\pi} \operatorname{Im} g(\mathbf{r}_0, \mathbf{r}_0, E). \tag{30}$$

Then the total energy of the point defect in the A-B-A sandwich system is obtained at 0K by

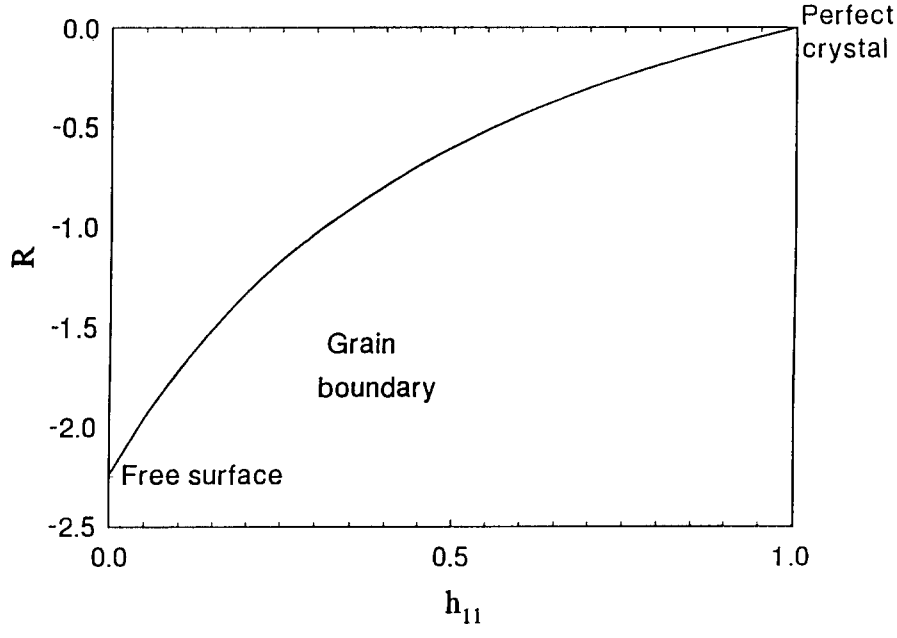

Fig. 2. Variation of R with the ratio of elastic constants, h_{11}, for a grain boundary thickness of 5 Å in aluminium.

summing $\epsilon(\mathbf{r}_0, E)$ over all possible states inside the Fermi surface

$$\epsilon(\mathbf{r}_0) = An(\mathbf{r}_0), \tag{31}$$

where $n(\mathbf{r}_0)$ is the electronic density at location $\mathbf{r}_0$

$$n(\mathbf{r}_0) = -\frac{1}{\pi} \operatorname{Im} \int^{E_F} dE g(\mathbf{r}_0, \mathbf{r}_0, E). \tag{32}$$

The calculation of the Green function is first performed in the two-dimensional space parallel to the interfaces by using the interface response theory [34]. This approach is similar to the one used in elasticity.

The Green function is again expressed as $g(\mathbf{k}_{//}; X_{03}, X_{03}; E)$ where $\mathbf{k}_{//}$ is the wave vector parallel to the interfaces and X_{03} is the position of the solute atom in the direction X_3 perpendicular to the interfaces. These expressions were derived in [36].

Finally, the electronic density is given by:

$$n(\mathbf{r}_0) = -\frac{1}{\pi} \operatorname{Im} \int^{E_F} dE \times \int \frac{d^2\mathbf{k}_{//}}{(2\pi)^2} g(\mathbf{k}_{//}; X_{03}; X_{03}; E). \tag{33}$$

In our calculation, the slab B and the perfect crystals A are characterized by their ground energies E_A, E_B and their effective masses m_A, m_B. In the nearly free electron model approximation, these parameters are related to the bulk electronic density n_i in metal i by the relation:

$$E_F - E_i = \frac{\hbar^2}{2m_i} \left(\frac{3n_i}{8\pi}\right)^{2/3}, \quad i = A, B. \tag{34}$$

The Fermi level of both metals are aligned in the sandwich system at the energy E_F. We also introduce the quantity

$$\alpha_i^2 = k_{//}^2 - \frac{(E - E_i)}{B_i} \quad \text{with} \quad B_i = \frac{2m_i}{\hbar^2} \tag{35}$$

For the sake of simplicity, we choose the effective mass of the electron to be the same in both media A and B ($B_A = B_B = B$). The electronic density in the system A-B-A parallels the atomic density. Therefore, we choose a lower electronic density for the slab as a representation of the lower atomic density within the core of a high-angle grain boundary. This is achieved by taking E_A below E_B.

The multiple integral in equation (33) can be simplified by the following change of variables:

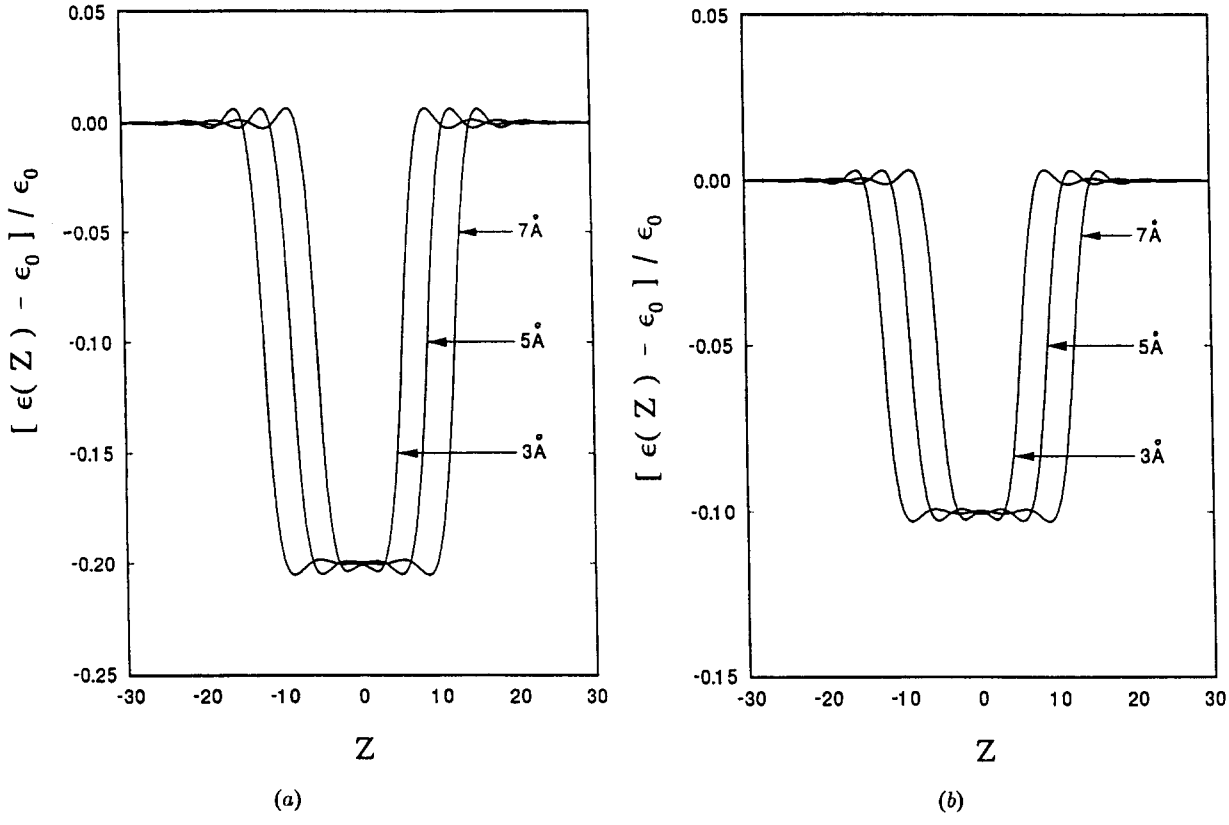

Fig. 3. Excess electronic energy near a grain boundary in a Al crystal, for three different thicknesses (3, 5, and 7 Å) of the grain boundary and for various atomic densities. The excess electronic energy is normalized to the electronic energy ϵ_0 of a solute atom in an infinite crystal of Al. The dimensionless quantity Z is equal to $2k_F X_{03}$, where k_F is the Fermi's wave vector of Al, and the electronic energy ϵ_0 is given by $\epsilon_0 = Ak_F^3/3\pi^2$. (*a*) $n_B/n_A = 0.8$; (*b*) $n_B/n_A = 0.9$.

$$v^2 = \frac{(E - E_i)}{B_1} - k_{//}^2 \tag{36}$$

and

$$w^2 = \frac{2m(E - E_1)}{\hbar^2} \tag{37}$$

and by inverting the order of integration over v and w. After some algebraic transformations, we obtain the electronic energy $\epsilon(\mathbf{r}_0)$ as a simple integral of the form

$$\epsilon(X_{03}) = \frac{A}{2\pi^2} \int_0^{k_F} (k_F^2 - v^2)\mathrm{Img}(v, X_{03})v dv. \tag{38}$$

We integrate the equation (38) numerically. In figure 3 the excess electronic energy of an impurity in the vicinity of a planar defect in aluminium for various thicknesses and atomic densities is reported.

This energy is proportional to the electronic density. Despite the absence of self-consistency in our calculations, they reproduce quite faithfully electronic densities for an identical planar defect in aluminium obtained with a self-consistent density functional formalism [26]. The amplitude of oscillations is more pronounced within our approximate method.

Outside the planar defect, the excess electronic energy exhibits an attenuated sinusoidal variation changing sign every fraction of an interatomic distance. This energy does not provide a strong driving force for segregation of impurities outside the slab. Strong variations in energy occur at the interfaces between the slab and the infinite media. The electronic driving force will give rise to a very local segregation. We define the solute/grain boundary binding electronic energy as the excess electronic energy within the core

of the planar defect. We may further take it as the average excess energy equal to $A(n_B - n_A)$ in view of the weak oscillations of the excess energy in the slab. This binding energy is insensitive to the thickness of the slab for thicknesses over 2 Å. In contrast, the excess electronic density in the core differs drastically from the atomic density for thicknesses less than 2 Å [36]. This results from an overlap of electronic density profile at the slab/infinite media interfaces. In consequence for thin grain boundaries, a reduction in binding energy is expected.

Contrary to the elastic binding energy, which is indirectly linked to the grain boundary density through the elastic constants, the electronic binding energy is directly related to the atomic density in the grain boundary core through a simple linear relation.

We can estimate the electronic contribution to the ratio R defined in the preceding section. The electronic contribution to the solubility limit is approximated by $\exp[-An_A/k_BT]$ yielding an expression for R in the form: $R = (n_B - n_A)/n_A$. For a grain boundary with 10% excess volume, R takes the value -0.1; a value very much lower than that predicted by the elastic model and measured by Hondros [9]. However, some caution is needed. The expression for the solubility limit is valid only in the case of solute atoms with low solubility [27]; an approximation incompatible with the first-order perturbation approach to calculating binding energies. Nevertheless, this result suggests that elastic effects dominate the phenomenon of segregation.

5. Conclusion

We have investigated the effect of thickness and atomic density of high-angle grain boundaries on solute segregation. Two simple models have been derived to account for the elastic and electronic contributions to the driving force for segregation. The electronic model is limited to the description of simple metals, and we restrict our elastic model to isotropic media. Furthermore, the electronic model is applied to solutions of heterovalent metals, and the elastic model accounts for the size effects in metallic alloys of isovalents metals.

The propensity for segregation of the grain boundary is characterized by the solute/interface binding energy. In the case of elasticity, we are able to calculate a correlation between the grain boundary enrichment factor and the atomic solid solubility in the limit of low solubility. This correlation is in excellent agreement with experimental observations of segregation in various metallic systems.

Grain boundary enrichment does not vary significantly with grain boundary thickness in the range of typical values for high-angle grain boundaries; this independently of the nature of the driving force for segregation.

On the other hand, the atomic density of grain boundaries plays an important role in segregation of impurities. The electronic binding energy depends explicitly on the atomic density. An elastic driving force exists for grain boundaries with elastic properties strongly tied to density. We have also considered the case of grain boundaries with atomic densities approaching the bulk value.

A high-angle grain boundary with near-bulk density in simple metals exhibiting large variations of elastic constants with density will show a small electronic segregation binding energy and an important elastic-binding energy. This may be the case for special grain boundaries in some metals. Since Wolf [16] has shown that the energy of high-angle grain boundaries increases linearly with the excess volume, high-density boundaries also corresponds to low-energy interfaces. This observation and our simple models suggest that segregation may occur to low-energy grain boundaries. This result is consistent with the Gibbs adsorption isotherm equation in which a partial derivative of energy with respect to chemical potential of the solute atom, and not an absolute energy, determines the solute excess. We conclude that although low density is sufficient for segregation, it is not a necessary condition. Moreover, grain boundaries with small excess volume may show a high adsorptive capacity.

Finally, we note that the change in density of the material at the grain boundary on which our model is based constitutes only one of the possible contributions to segregation. Internal stresses developing in the vicinity of the grain boundary due to its atomic structure will inter-

act with the impurity's stress field. In another publication [37] we have modeled the stress field around a high-angle grain boundary by a two-dimensional array of compressive forces. It is shown that periodicity in the stress field annihilates the effect of the local sources of stress in the boundary as a driving force for segregation, leaving density as the most important effect for periodic high-angle grain boundaries.

Appendix

We give in this appendix the expression of the function $\Phi(k_{//})$ defined in equation (20).

$$\Phi(k_{//}) = \frac{1}{2}(A^S + A^A + H^S + H^A) \tag{39}$$

where the $A^{S,A}$ and $H^{S,A}$ are given by

$$A^{S,A} = \frac{\alpha^3 + \alpha^2 C^{S,A}\cosh(2ak_{//}) - 2\alpha D^{S,A}}{2D^{S,A}} \tag{40}$$

$$H^{S,A} = \frac{\alpha^2 E^{S,A}}{D^{S,A}} \tag{41}$$

with: $\nu = C_{44}/C_{11}$; and $\nu' = C'_{44}/C'_{11}$

$$\alpha = -\frac{4k_{//}C_{44}}{1+\nu} \tag{42}$$

$$C^{S,A} = \frac{\pm 2C'_{44}k_{//}}{ak_{//}(1-\nu') \mp \frac{1}{2}(1+\nu')\sinh(2ak_{//})} \tag{43}$$

$$D^{S,A} = \frac{\alpha^2}{4} + \frac{(C^{S,A})^2}{4}[\cosh^2(2ak_{//}) - 1] + \frac{\alpha}{2}C^{S,A}\cosh(2ak_{//}) - (E^{S,A})^2 \tag{44}$$

$$E^{S,A} = \frac{\alpha\nu}{2} + C^{S,A}[\pm(1-\nu')ak_{//} - \frac{\nu'}{2}\sinh(2ak_{//})] \tag{45}$$

Acknowledgments

The major part of this work was done at the University of Arizona during a stay of J.O. Vasseur. J.O. Vasseur would like to thank the Université des Sciences et Technologies de LILLE for financial support.

References

1. H.L. Marcus, L.H. Hackett Jr., and P.W. Palmberg, "Temper Embrittlment of Alloy Steels," *STP 499, 90* (American Society for Testing and Materials, Philadelphia, 1972).
2. J.G. Hu and D.N. Seidman, Phys. Rev. Letts, **65**, 1615 (1990).
3. H.C. Lin, Cornell University Diss. Abstr. Int. **51(2)**, 200 (1990).
4. J. Friedel, 4ème Colloque de Metallurgie, Saclay, Presses Universitaires de France **95** (1960).
5. S. Suzuki, K. Abiko, and H. Kimura, Scripta Metall. **15**, 475 (1987).
6. D. Bouchet and L. Priester, Scripta Metall. **21**, 475 (1987).
7. G. Herrmann, H. Gleiter, and G. Bärö, Acta Metall. **24**, 353 (1976).
8. H. Sautter, H. Gleiter, and G. Bärö, Acta Metall. **25**, 467 (1977).
9. E.D. Hondros, J. Phys. (Paris) **36**, C4-117 (1975).
10. M.P. Seah and E.D. Hondros, Proc. R. Soc. Lond. A **335**, 191 (1973).
11. D. McLean, in *Grain Boundaries in Metals* (Oxford University Press, London, 1957), p. 116.
12. A. Brokman, Acta Metall. **35**, 307 (1987).
13. W.L. Alba and K.B. Whaley, J. Chem. Phys. **95**, 4427 (1991).
14. H.K. Chang, J.K. Lee, and D.F. Stein, in *Interatomic Potentials and Crystalline Defects,* edited by J.K. Lee Metallurgical Society of AIME, 373 (1980)
15. S.M. Foiles, Phys. Rev. B **40**, 11502 (1989).
16. D. Wolf, J. Mater Res. **5**, 1708 (1990).
17. J. Friedel, Advances in Physics **3**, 446 (1954).
18. B.J. Pines, J. Phys. U.S.S.R. **3**, 309 (1940).
19. G. Leibfried and N. Breuer, in *Point Defect in Metals,* vol. 1, (Springer, Berlin 1978), p. 145.
20. A.A. Maradudin and R.F. Wallis, Surf. Science **91**, 423 (1980).
21. P. Deymier, L. Janot, J. Li, and L. Dobrzynski, Phys. Rev. B **39**, 1512 (1989).
22. B. Djafari-Rouhani, L. Dobrzynski, and R.F. Wallis, Phys. Rev. B **16**, 741 (1977).
23. J.D. Eshelby, *Solid State Phys.,* vol. 3 edited by F. Seitz and D. Turnbull, (Academic Press New York 1956), p. 79.
24. Yu. A. Kosevich, Sov. Phys. JETP **54**, 1193 (1981).
25. R.W. Balluffi, in *Interfacial Segregation,* edited by W.C. Johnson and J.M. Blakely (American Society for Metals 1979), p. 193.
26. J.R. Smith and J. Ferrante, Phys. Rev. B **34**, 2238 (1986).
27. M.P. Seah, J. Phys. F: Metal Phys. **10**, 1043 (1980).
28. A.A. Maradudin, unpublished work.
29. G. Simmons and H. Wang, *Single Crystal Elastic Constants and Calculate Aggregate Properties. A Handbook,* second edition, (M.I.T. Press, Cambridge, MA, 1971).
30. D. Wolf and J.F. Lutsko, J. Mater. Res. **6**, 1427 (1989).
31. S. Brunauer, P.H. Emmett, and E. Teller, J. Am. Chem. Soc. **60**, 309 (1938).
32. B. Djafari-Rouhani, L. Dobrzynski, A.A. Maradudin, and R.F. Wallis, Surf. Science **91**, 618 (1980).

33. P. Guyot and J.P. Simon, J. Phys. (Paris) **36**, C4–141 (1975).
34. L. Dobrzynski, Surf. Science **180**, 505 (1987); L. Dobrzynski, Surf. Science **200**, 435 (1988).
35. G. Allan, Annales de Phys. **5**, 169 (1970).
36. J.O. Vasseur, P.A. Deymier, A. Akjouj, L. Dobrzynski, and B. Djafari-Rouhani, Acta Physica Polonica A **81**, 39 (1992).
37. J.O. Vasseur and P.A. Deymier, to be submitted to Interface Science.